

Cite this: *Green Chem.*, 2021, **23**, 3039

Auto-tandem PET and EnT photocatalysis by crude chlorophyll under visible light towards the oxidative functionalization of indoles†

Saira Banu,^{a,b} Shubham Choudhari,^a Girija Patel^{a,b} and Prem P. Yadav  ^{*a,b}

Chlorophyll is the most abundant photocatalytic pigment that enables plants to absorb solar energy and convert it to energy storage molecules. Herein, we report a tandem photocatalytic approach utilizing the natural pigment chlorophyll in crude form to achieve photoinduced electron transfer (PET) and energy transfer (EnT) towards the oxidative functionalization of indoles. Redox potentials, ESR, fluorescence quenching and UV experiments have evidenced the dual catalytic activity of chlorophyll. The highlight of the study is the auto-tandem photocatalytic role of chlorophyll to enable the green oxidation of indoles using molecular oxygen as the oxidant, water as the reaction medium, and photochemical energy from the visible region of the spectrum.

Received 13th January 2021,
Accepted 17th March 2021

DOI: 10.1039/d1gc00138h

rsc.li/greenchem

Introduction

The sustainability aspects of organic syntheses have become the prime objective with nature being the foremost inspiration in this regard. Solar radiations have been the ultimate source of light and energy on earth.¹ Also, they are the most abundant, inexpensive and renewable source of green energy.² The high energy UV region of the light is mostly absorbed by organic molecules and hence has been most widely used in organic syntheses;³ however, limited by its harsh nature, safety issues and requirement of special photoreactors. Thus, it is much needed to utilize the wavelength of visible light abundant in the solar spectrum.⁴ Visible light photocatalytic applications have started to emerge in the recent past and provide a greener, cleaner, and more sustainable approach towards multiplying the organic chemical space.⁵ The ultimate goal to match the ability of nature to harness solar energy by its photosynthetic machinery has led to several discoveries in the field of synthetic photochemistry and the quest is still on.⁶ Mostly, transition metal-based polypyridyl complexes are used for visible light-mediated reactions; simultaneously, organic dyes are gaining momentum as the photocatalyst of choice.⁷ Organic photoredox catalysts have existed for long; however, their role as a PET^{6a} catalyst in organic syntheses has seen

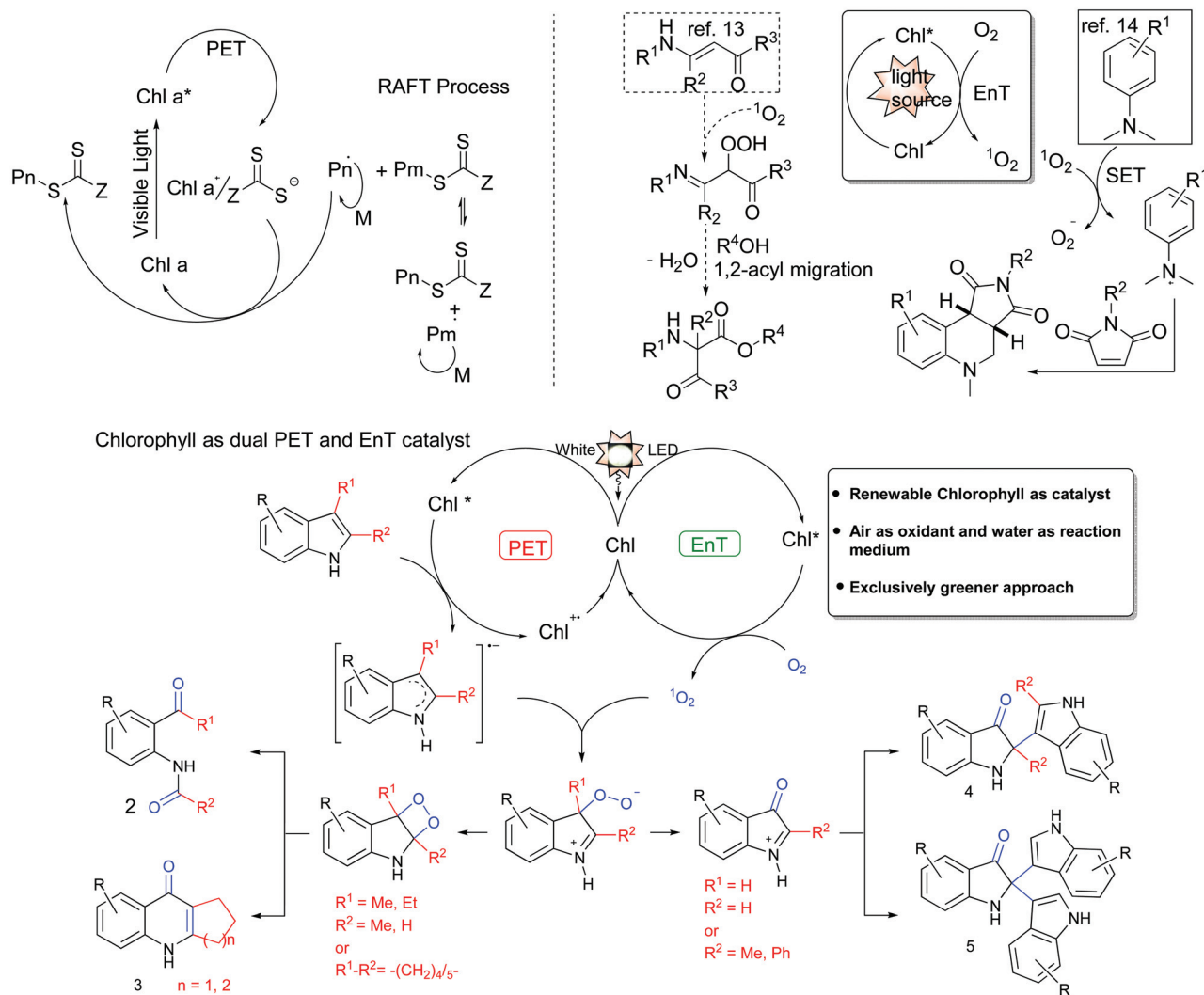
encouraging growth in the recent past. The green pigment “chlorophyll” in the leaves of plants has been the key source of inspiration to the community working on photochemical reactions,⁸ and the ultimate aim of mimicking the natural phenomenon of photosynthesis has gained much needed attention to achieve sustainability.

Chlorophyll is known to be involved in the PSI and PSII processes *via* energy transfer (EnT)⁹ and photoinduced electron transfer.¹⁰ Surprisingly, in the context of visible light-mediated synthetic reactions, the use of chlorophyll as a photocatalyst remains quite unexplored. The isolation, purification, and stability of the natural pigment chlorophyll may have contributed to its scarce exploration as the photocatalyst. In the recent past, some visible light-mediated transformations utilized chlorophyll as a photocatalyst.¹¹ Some of these reports have outlined a detailed mechanistic proposal. Boyer *et al.* reported the chlorophyll a catalyzed electron transfer mechanism to enable controlled radical polymerization under visible light; they have achieved the same feat even with the crude extract of chlorophyll a (Scheme 1a).¹² Furthermore, the photo-degradability of chlorophyll in the air to polar components shunned the need for catalyst removal, making the purification process easier.^{12b} Very recently, Das *et al.* reported chlorophyll-catalyzed singlet oxygen generation *via* EnT, followed by 1,2-acyl migration reactions to achieve α -amino carbonyl compounds from the corresponding hydroperoxides (Scheme 1b).¹³ In another report, the EnT-generated singlet oxygen undergoes SET with the substrate, which ultimately got converted to tetrahydroquinolines (Scheme 1b).¹⁴ Most of these reactions use either PET or EnT properties of the photocatalyst chlorophyll, whereas ground state redox potentials were mentioned to sub-

^aMedicinal and Process Chemistry Division, CSIR-Central Drug Research Institute, Lucknow-226031, India. E-mail: pp_yadav@cdri.res.in

^bAcademy of Scientific & Innovative Research, Ghaziabad-201002, India

†Electronic supplementary information (ESI) available: Synthetic procedures, mechanistic investigations, characterization data and ¹H, ¹³C NMR spectra of synthesized compounds. See DOI: 10.1039/d1gc00138h

(a) Chlorophyll as PET catalyst (Boyer *et al.*, 2015 & 2017)¹² (b) Chlorophyll as EnT catalyst (Das *et al.*, 2020, and He *et al.*, 2017)¹³⁻¹⁴

Scheme 1 Chlorophyll as a mechanistically defined photocatalyst.

stantiate the mechanistic proposals. However, the excited state redox potentials of chlorophyll a calculated as per Nicewicz *et al.*^{6a} and ground state redox potentials¹⁵ were found to be E_{oxd}^* (singlet state) = -1.04 V vs. SHE , E_{oxd}^* (triplet state) = -0.53 V vs. SHE , and E_{red}^* (singlet state) = 0.73 V vs. SHE , E_{red}^* (triplet state) = 0.22 V vs. SHE (section 3.3A, ESI†). Accordingly chlorophyll a could act as an efficient photoredox catalyst as E_{oxd}^* (cat^{+/}/cat*) < 0; E_{red}^* (cat*/cat⁻) > 0.^{6a}

Previous work

Henceforth, we lend credence to the fact that with proper designing, chlorophyll a with appropriate excited state redox properties and triplet state excitation energy $E_T = 30.9 \text{ kcal mol}^{-1}$ (ref. 16) may act as an efficient photocatalyst. Herein, we report the oxidative functionalization of indoles *via* the auto-tandem photocatalysis *viz.*, PET and EnT under the visible-light excitation of the crude chlorophyll (Scheme 1c), enabling the 2,3-substitution-driven diverse array of products *via* the key

PET-mediated reduction of indole to indolyl radical anion species, followed by reactions with EnT-derived singlet oxygen. The oxidative cleavage of indoles¹⁷ is one of the fundamental transformations found to be involved in the peroxidase-catalyzed transformation of L-tryptophan to L-formylkynurenine, leading to the amino acid kynurenine, and it also happens to be the first key step in the biosynthesis of coenzyme NAD.¹⁸ The oxidative cleavage of 2,3-dimethylindoles generates *N*-acetylaminoacetophenones (and their downstream products 2'-aminoacetophenones), which are the key starting materials for the synthesis of different biologically active molecules and drugs such as linagliptin.¹⁹ Witkop oxidation^{17a,18b} is the most prevalent and general method for the oxidative cleavage of indoles to *N*-acetylaminoacetophenones. Besides this method, ozonolysis²⁰ and a very recent ozone-halide catalysis system was reported to effect the transformation efficiently.²¹ Conventional methods usually require organic oxidants or toxic transition metals, which produce harmful by-products.

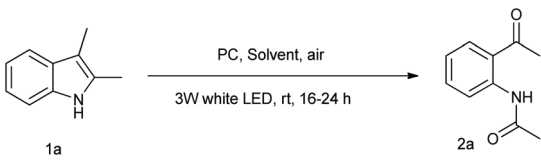
Therefore, it is highly desirable to develop a benign, efficient reaction protocol using safer oxidants and solvents. In addition, the synthetic applicability of the downstream products and our interest in the synthetic exploration of substituted 2'-aminoacetophenones and indoles²² led to the selection of substituted indoles as substrates to study the Chl-mediated oxidative functionalization. This natural pigment chlorophyll (crude extract) catalysis system can offer a general, sustainable, green oxidation process for indoles, evading the use of hazardous oxidants, and provide better atom economy than other reported methods.

Results and discussion

First, 2,3-dimethylindole (**1a**) was selected as the model substrate and crude chlorophyll (c-Chl) derived from spinach was used as the photocatalyst. The determination of chlorophyll a concentration in crude extract was done *via* UV-Vis spectroscopy based on the Wellburn equation²³ (Fig. FS1, ESI†). As shown in Table 1, a preliminary screening was conducted with **1a** using c-Chl (Chl a, 30 ppm) as the photocatalyst, CH₃CN (5 mL), in an air atmosphere, under the irradiation of 3 W white LED at room temperature. The desired product *N*-(2-acetylphenyl)acetamide (**2a**) was obtained with a satisfactory yield of 64% (entry 1). The role of Chl a as the catalyst in the crude form was substantiated by carrying out the reaction with pure Chl a. A similar result was obtained (entry 2, 62%) as compared to the crude chlorophyll. Thereafter, switching the catalytic system from c-Chl to other commonly used photosensitizers, *viz.* methylene blue (MB), eosin Y (EY), rose Bengal (RB) resulted in a reduced yield of **2a** (entries 3–5). Next, the optimization of solvents was performed (entries 1, 6–10). The solvents in which substrate **1a** and photocatalyst c-Chl were readily soluble, such as MeCN, MeOH, DMSO, and DMF, afforded good to moderate yields. Next, to screen water as a solvent, MeOH-water (1 : 10) was used (**1a** and c-Chl were insoluble in water) and it provided 69% yield of **2a** (entry 9). To further elaborate water as the solvent system, H₂O/SDS was also used in the optimization (entries 10–19). Gratifyingly, H₂O/SDS provided a better product yield than the other solvents, although **1a** and c-Chl had low solubility in H₂O/SDS. Most probably, a low concentration of the substrate in the reaction solution may be favorable for the control of reaction rate, thereby leading to a relatively clean reaction.

Furthermore, higher concentrations of chlorophyll a are presumed to undergo self-quenching; therefore, the analysis of the effects of the Chl a concentration was carried out (entries 10–11, 13–14). The Chl a concentration of 15 ppm provided the highest yield within reduced time as compared to that of 30 ppm. As per literature reports,^{12a,24} fluorescence intensity decreases at higher concentrations of Chl a due to the fast transfer of excitation energy to the statistical pairs of Chl a present in close vicinity with each other in the solution. However, further lowering the Chl a concentration to 10 ppm (entry 13) and 5 ppm (entry 14), afforded product **2a** in com-

Table 1 Optimization of conditions for the visible light-mediated photo-oxidative functionalization of 2,3-dimethylindole(s) (**1a**) to *N*-(2-acetylphenyl)acetamide (**2a**)^a



Entry	Solvent	PC	PC (Conc.)	Time (h) ^b	Yield (%) ^c
1	MeCN	c-Chl	30 ppm	24	64
2	MeCN	Chl a	30 ppm	16	62
3	MeCN	EY	5 mol%	24	17
4	MeCN	MB	5 mol%	24	15
5	MeCN	RB	5 mol%	24	26
6	MeOH	c-Chl	30 ppm	24	67
7	DMSO	c-Chl	30 ppm	24	53
8	DMF	c-Chl	30 ppm	24	39
9	MeOH : H ₂ O(1 : 10)	c-Chl	30 ppm	16	69
10	H ₂ O/SDS	c-Chl	30 ppm	24	83
11	H ₂ O/SDS	c-Chl	15 ppm	18	90 (79 ^d)
12	H ₂ O/SDS ^e	c-Chl	15 ppm	28	87
13	H ₂ O/SDS	c-Chl	10 ppm	24	54
14	H ₂ O/SDS	c-Chl	5 ppm	24	37
15 ^f	H ₂ O/SDS	c-Chl	15 ppm	24	63
16 ^g	H ₂ O/SDS	c-Chl	15 ppm	36	67
17 ^h	H ₂ O/SDS	c-Chl	15 ppm	48	NR
18	H ₂ O/SDS	—	—	48	Trace
19 ⁱ	H ₂ O/SDS	c-Chl	15 ppm	24	85
20 ^j	MeOH(dry)	c-Chl	15 ppm	48	NR

^a Reaction conditions: Air atmosphere and irradiation of visible light with 3 W white LED, 2,3-dimethyl indole (**1a**) (0.2 mmol, 1 equiv.), photocatalyst (PC) solvent (5–10 ml), SDS (1 equiv.), temperature (RT, approx. 25 °C), time (16–24 h) in a 30 mL glass vial. ^b Time for the consumption of the substrate as per TLC observation. ^c Conversion yields were determined by ¹H NMR using dibromomethane as the internal standard. ^d Isolated yield. ^e SDS (0.5 equiv.). ^f The reaction was performed under irradiation of 3W blue LED. ^g The reaction was performed under irradiation of 3W red LED. ^h No light. ⁱ Reaction performed under oxygen atmosphere instead of air. ^j Argon atmosphere instead of air. NR = No reaction. PC = photocatalyst.

paratively low yields. Chlorophyll a possesses two prominent absorption bands at 430 nm (Soret band, blue region) and at 665 nm (Q-band, red region) of the visible spectrum. However, the reaction under the irradiation of 3 W blue and red LEDs (entries 15 and 16) further reduced the yield of product **2a**. The broad spectrum of wavelength (400–700 nm) in the case of white light^{11c,25} comprising both the significant regions of Chl absorption bands, *viz.*, 350–450 nm and 650–700 nm, may be required for efficient PET and EnT processes. There was no significant conversion in the absence of light (entry 17); however, without photocatalyst c-Chl, a trace amount of the product was obtained (entry 18). Furthermore, the reaction under oxygen atmosphere resulted in an almost similar yield as that under air atmosphere (entry 19); however, no product was observed under an argon atmosphere (entry 20). Furthermore, as per our observations and literature reports, Chl is degraded to unreactive polar species,²⁶ simplifying the final removal of photocatalyst from the reaction mixture.^{12b}

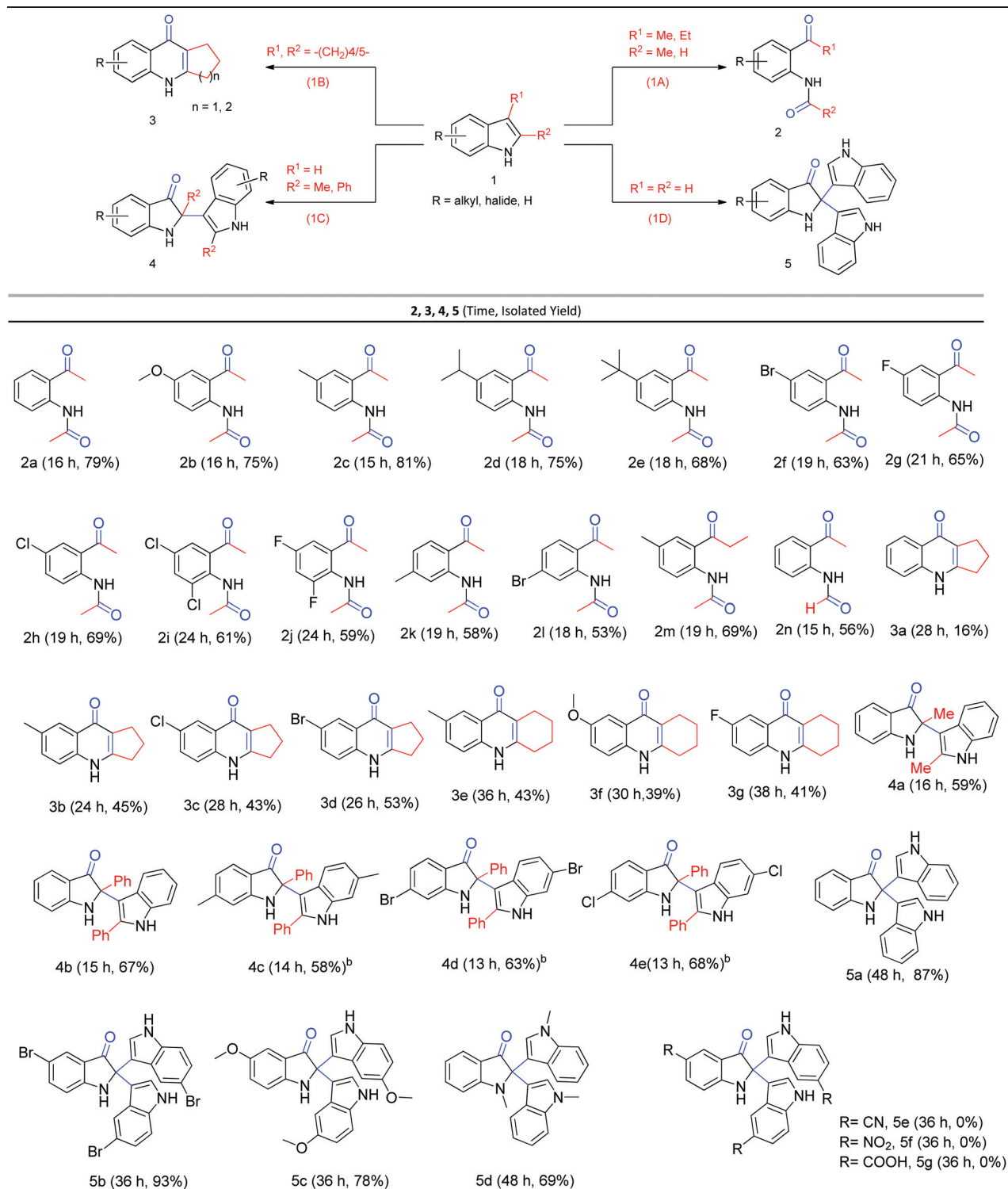
With the determination of the optimized condition for visible light-mediated aerobic oxidation conditions, the substrate scope of indoles was assessed. It was delightful to witness the reaction method's versatility with indole moieties, which were either commercially available or synthesized following literature methods,²⁷ affording mechanistically divergent products based on the substitutions of indole on 2,3-positions (Table 2). Indole-bearing alkyl substitution at C-2,3 (**1a-m**) and C-3 (**1n**) smoothly undergo photo-oxidative cleavage rendering *N*-(2-acetylphenyl)acetamides (**2a-m**), *N*-(2-formylphenyl)acetamide (**2n**) in good to moderate yields. On the other hand, 3-acetylindole did not react under optimized conditions. 2,3-Dimethylindole-bearing electron-donating groups (-OMe, -Me, -ⁱPr *etc.*) and electron-withdrawing groups (-Br, -Cl, -F *etc.*) on the phenyl ring exhibited adequate reactivity and afforded the corresponding oxidized products (**2b-e**, **2k**) and (**2f-j**, **2l**) in good to moderate yields. The reaction time was mainly dependent on the comparative ease of substrate-solubility in the water-SDS system. Subsequently, the reactivity of differently substituted tetrahydrocarbazoles and hexahydrocyclohepta[*b*]indole (**1B**) was investigated, and they were found to undergo photooxidative functionalization to fused quinolones, and 1,2,3,4-tetrahydroacridin-9(10*H*)-ones²⁸ (**3**), respectively, in 10–15% isolated yields. Such type of an indole-quinolone rearrangement was reported by Winterfeldt,^{18b,29} who found out different conditions that could accomplish the one-pot Witkop oxidation, followed by Camps cyclization to provide quinolones, which widely exist in numerous marketed drugs and bioactive molecules.³⁰ After going through screening of different bases and acids (Table TS1, ESI†), it was observed that 1 equiv. of K₃PO₄ in addition to the optimized condition for 2,3-dimethyl indoles afforded the Witkop-Winterfeldt products (**3a-g**, Table 2) in moderate yields. On the other hand, the indole-bearing substitutions at C-2 only (**1C**) underwent oxidative dearomatization instead of photooxidative cleavage, attaining 2-indole-substituted 3-oxindoles (**4**) with 43% yield. Herein, also the addition of 0.5–1.0 equiv. of base (K₃PO₄ or Cs₂CO₃) resulted in the enhancement of yield (60–65%) of the desired products (**4a-e**). Mass spectrometry of the crude mixture indicated the presence of 2-substituted indolin-3-one (section 2.2A, ESI†), suggesting the involvement of *in situ* generated iminium species as an intermediate.³¹ Similarly, C-2,3 unsubstituted 1*H*-indoles and 1-methyl-1*H*-indole, under the same reaction condition, yielded corresponding 2,2-bis(indol-3-yl)indolin-3-ones (**5a-d**) in a regioselective manner. Indole-bearing electron-donating and moderately electron-withdrawing functionalities on the phenyl ring afforded the products in good to excellent yields, while the strong electron-withdrawing group (-CN, -NO₂, -COOH)-containing indoles remained unreacted (**5e-g**, Table 2). Furthermore, the absence of the product 3,3-bis(indol-3-yl)indolin-2-one implied that isatin, proposed as an intermediate by Thakur *et al.*,³² was not involved in the present study. The observation also substantiated the proposed mechanism indirectly (Scheme 2). In the case of 1-methyl-1*H*-indole, the reaction needs to be continued for more than 48 h and an

excess of *c*-Chl a (Chl a = 10 ppm) was required. It could be envisaged that indole *N*-Me protection rendered it less prone to the oxidative quenching of excited Chl at the initial step (see plausible mechanism; Scheme 2), thereby decreasing its reactivity. So far, there are several reports for the synthesis of C-2 quaternary indolinones,^{31,33} the majority of them utilized a specialized metal catalyst, high temperature, external oxidant *viz.*, peroxides (TBHP). The present visible light-mediated *c*-Chl catalyzed system could provide a benign, useful strategy for the synthesis of 2-(indol-3-yl) indolin-3-one and 2,2-bis(indol-3-yl)indolin-3-ones from their corresponding indoles. Overall, the findings suggest that indoles' photooxidative functionalization is highly substrate selective with respect to the C2-C3 substitution patterns, leading to diverse products. The protocol developed herein afforded better chemo and regioselectivity, alleviating the need of indole *N*-H protection, which seems to be prerequisite in earlier methods.^{17b,c}

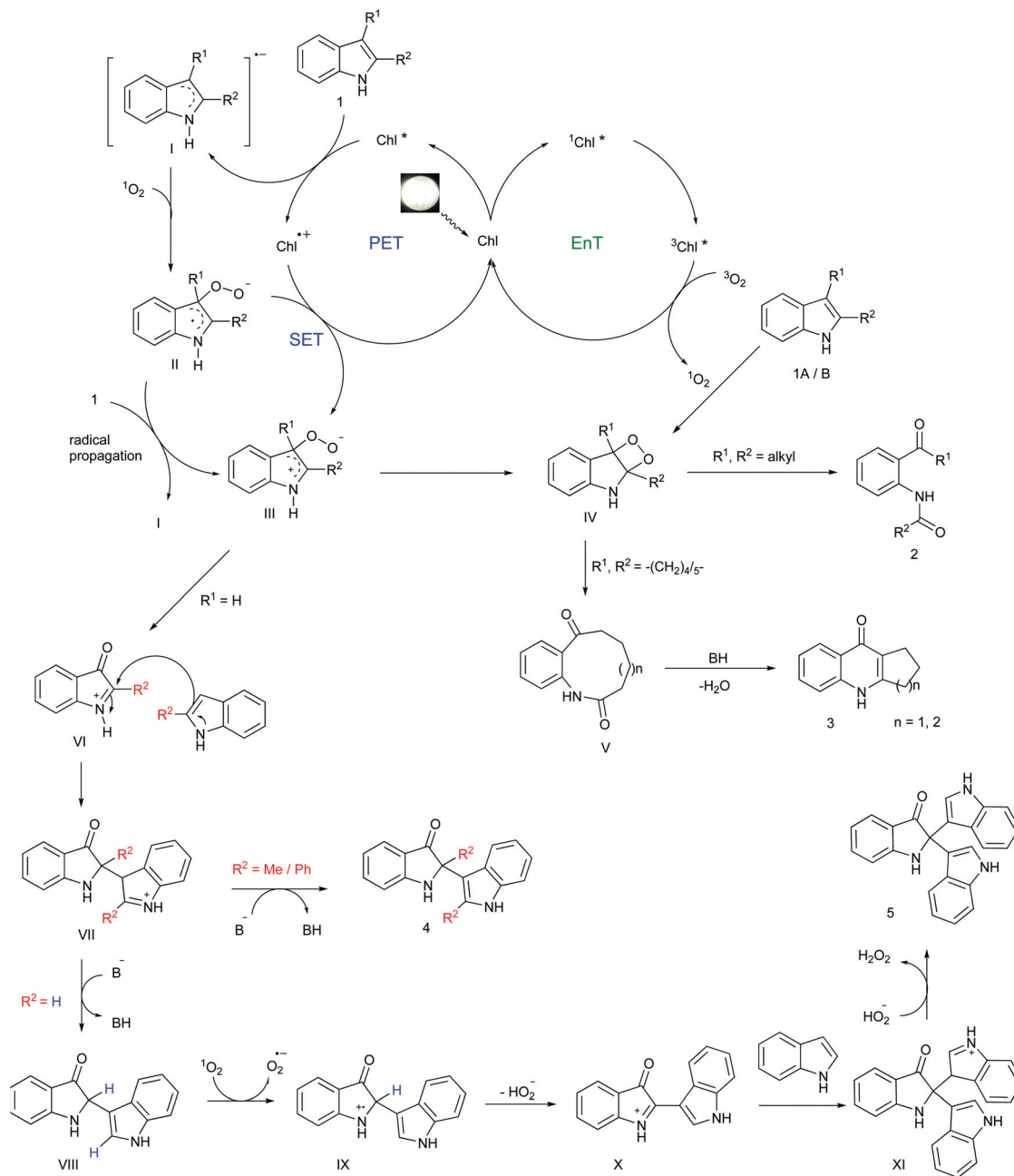
A gram scale reaction was performed with 2,3-dimethylindole (**1a**) (1.5 g) under optimized reaction conditions to demonstrate the present visible light-mediated method's synthetic workability. It provided the desired product *N*-(2-acetylphenyl)acetamide (**2a**) with 69% yield (1.27 g).

Mechanistic investigations

Next, to delve into the mechanism, some control experiments were performed using 2,3-dimethylindole (**1a**) as the model substrate. When 2,2,6,6-tetramethylpiperidinoxy (TEMPO) or 2,6-di-*tert*-butyl-4-methylphenol (BHT) was added to the reaction under optimized conditions, the yield of **2a** decreased significantly (Fig. 1a). It indicated that the reaction might involve radical generation (Fig. FS2a and b, ESI†). On the other hand, the use of 1,4-diazabicyclo [2,2,2]octane (DABCO) and sodium azide, both singlet oxygen quenchers (Fig. 1b), made the reaction sluggish, with the reduction in yield of **2a** (Fig. FS2c and d, ESI†). The addition of both radical quenchers (TEMPO and BHT) and singlet oxygen quenchers (DABCO and NaN₃) resulted in a significant decrease in the yield of **2a**; this led to hypothesize that the reaction follows both PET and EnT processes. The formation of electron donor-acceptor (EDA) complexes between chlorophyll (PC) and indoles was ruled out *via* UV-Vis spectroscopy of **1a** and PC in DMSO (FS11, ESI†). Next, Stern-Volmer fluorescence quenching experiments were carried out, (Fig. FS3, ESI†). When the chlorophyll-DMSO solution was excited at 433 nm, a 671 nm fluorescence was observed, and bubbling oxygen through the photocatalyst-DMSO solution did not have any significant effect on the fluorescence intensity (Fig. FS6, ESI†). However, on adding 2,3-dimethylindole, the photocatalyst fluorescence intensity decreased significantly (Fig. 1c and d and Fig. FS4 and 5, ESI†). These results suggest that the excited Chl initiates single-electron transfer with the quencher. The observation was further supported by redox potential values of the catalyst and substrate, as $E_{1/2 \text{ red}}$ of 2,3-dimethylindoles were found to be +0.087 V *vs.* SHE (see Fig. FS7, ESI†), which is higher than

Table 2 Substrate scope for the Visible light-mediated photo-oxidative functionalization of 2,3-dimethylindoles and related N-heterocycles^{a,b}

^a Reaction conditions: Air atmosphere and irradiation of visible light with 3 W white LED, indole (**1A**, **1B**, **1C**, **1D**) (0.2 mmol, 1 equiv.), photo-catalyst crude chlorophyll extract (Chl a = 15 ppm), solvent (water, 10 ml), SDS (0.2 mmol, 1 equiv.) temperature (RT, approx. 25 °C), time (10–48 h) in a 30 mL glass vial. K₃PO₄ (0.1–0.2 mmol, 1 equiv.) was added in case of **1B**, **1C**, and **1D**. ^b Reaction performed with CH₃CN (5 mL), Cs₂CO₃ (0.2 mmol, 1 equiv.).



Scheme 2 Plausible mechanism.

the $E_{1/2 \text{ oxd}}$ of triplet excited chlorophyll a, *i.e.*, -0.53 V vs. SHE (-1.04 V vs. SHE for the singlet excited state of chlorophyll a).^{6a,15,16} However, for molecular oxygen to get reduced to superoxide ion $\text{O}_2^{\bullet-}$, the potential was reported to be -1.23 V vs. SCE .^{17c} Hence, there would not be any admissible single electron transfer between the triplet excited state of Chl a and molecular oxygen. Furthermore, the Stern Volmer fluorescence quenching experiment performed with molecular oxygen (Fig. FS6; ESI†) is in line with the aforementioned redox potentials. On the other hand triplet state energy (theoretical value) of chlorophyll a was reported to be $30.9 \text{ kcal mol}^{-1}$ (1.34 eV),¹⁶

which implies that the triplet photosensitization of $^3\text{O}_2$ to $^1\text{O}_2$ [$E(1\Delta - 3\Sigma) = 22.5 \text{ kcal mol}^{-1}$],^{17c} by $^3\text{Chl}^*$ is feasible. Further, to find out the photosensitized generation of $^1\text{O}_2$ under optimized reaction conditions, 1,3-diphenylisobenzofuran (DPBF) (6) was used to trap the *in situ* generated singlet oxygen. The reaction led to the isolation of the diketone product 1,2-phenylenebis(phenylmethanone) (7) with 69% yield, confirming the generation of $^1\text{O}_2$ in the operative EnT mechanism (see Fig. 2a and ESI†).

It was further substantiated by UV-Vis spectroscopy using DPBF (with a characteristic peak at 412 nm),³⁴ for detecting

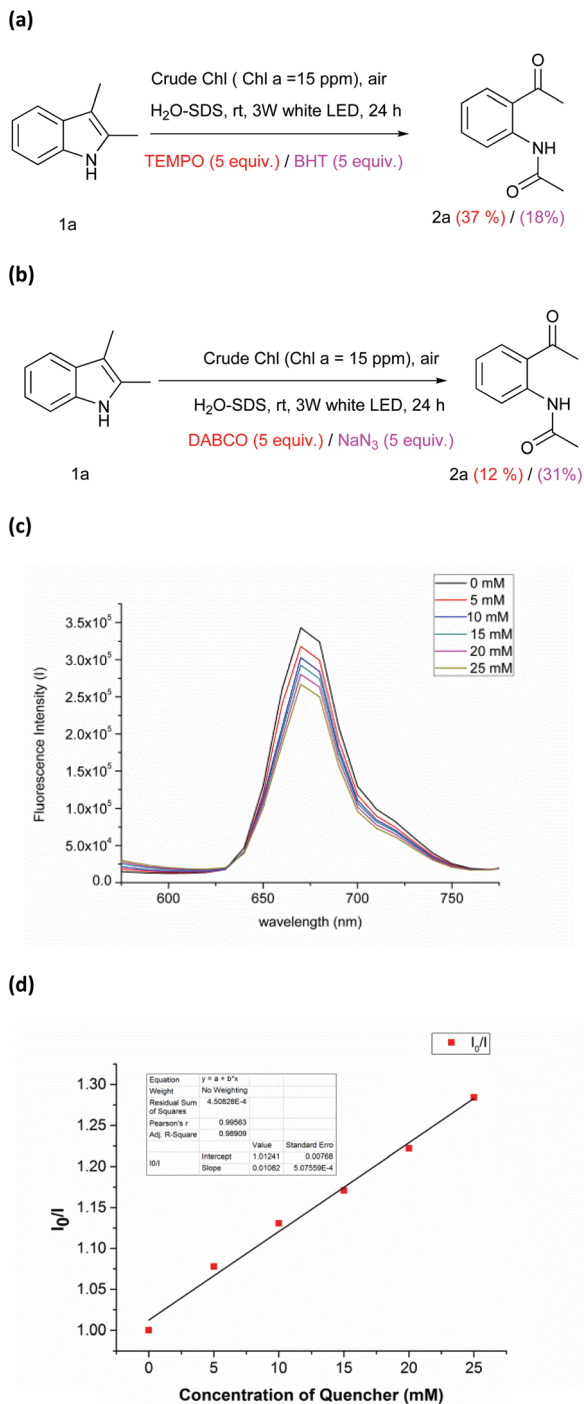


Fig. 1 (a) Control experiments performed with free radical scavengers TEMPO and BHT, respectively. (b) Control experiments performed with singlet oxygen quenchers DABCO and NaN₃, respectively. (c) Fluorescence emission spectra of **1a** (Chl a = 1 μM) with different concentrations of **1a** excited at 433 nm. (d) Linear fit plot of fluorescence quenching. The decrease in the emission intensity is correlated with the Stern–Volmer equation, $I_0/I = 1 + k_q\tau_0[Q]$, where I_0 and I are the emission intensity in the absence and presence of a quencher, k_q is the quenching rate constant, τ_0 is the excited lifetime, $[Q]$ is the quencher concentration.

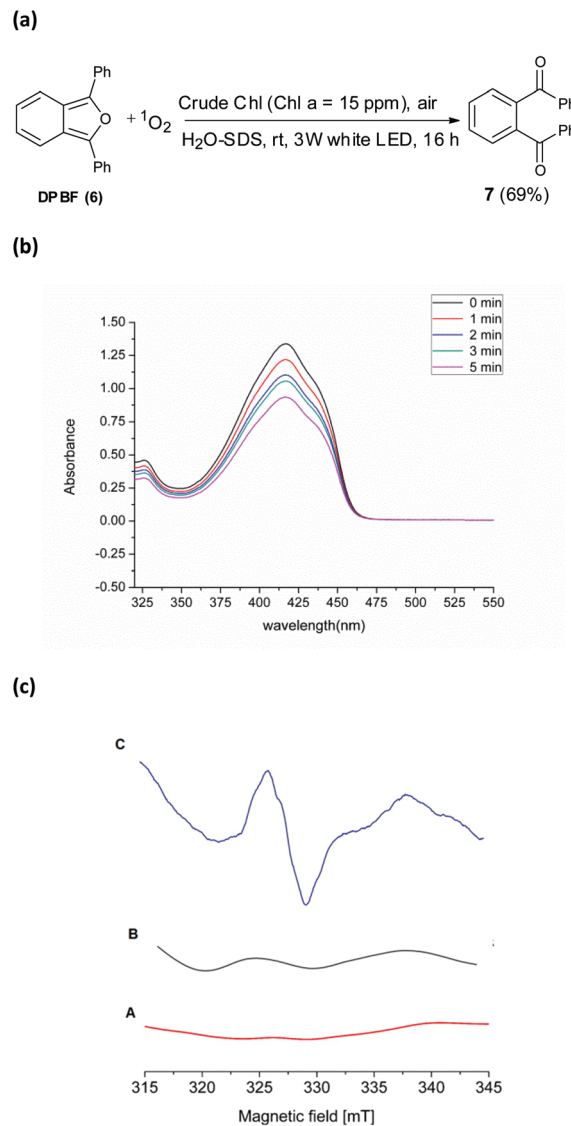


Fig. 2 (a) Diketone product 1,2-phenylenebis (phenylmethanone) (**7**) isolated from the reaction of DPBF (**6**) under optimised reaction condition. (b) UV-Visible experiment to investigate singlet oxygen generation; DPBF, PC, 3 W White LED. (c) (A) ESR spectrum of mixture of crude Chlorophyll a (PC), DMPO in DMSO under irradiation of 3 W white LED for 10 min. (B) ESR spectrum of the mixture of PC, **1a**, DMPO in DMSO under dark conditions for 10 min. (C) ESR spectrum of mixture of PC, **1a**, DMPO in DMSO under irradiation of 3 W white LED for 10 min.

singlet oxygen generation in the reaction medium. In the presence of light and photocatalyst, the intensity of DPBF gradually decreased with time (Fig. 2b and Fig. FS12, ESI†). The ESR study using 5,5-dimethyl-1-pyrroline *N*-oxide (DMPO) as the spin-trapping agent indicated the type of radical species or ROS involved in the reaction system (Fig. 2c).

A mixture of Chl a crude extract (containing Chl a concentration = 15 ppm), DMPO (0.7 mM) in DMSO was irradiated with 3 W white LED for 10 min under air atmosphere, and a small amount of the solution was transferred to a capillary. The ESR spectrum displayed no signal (Fig. 2c_A). Similarly, the

ESR spectrum for the mixture of Chl a crude extract (Chl a = 15 ppm), **1a** (0.7 mM), DMPO (0.7 mM) in DMSO without irradiation of visible light showed no signal (Fig. 2c_B). After irradiation with 3 W white LED for 10 min, the ESR spectrum for the mixture of Chl a crude extract (Chl a = 15 ppm), **1a** (0.7 mM), DMPO (0.7 mM) in DMSO, exhibited a new broad signal (Fig. 2c_C) without any detectable hyperfine splitting over a wide range of temperature ($g = 2.0024$, with epr line width = 9 Gauss). The signal may correspond to the pi-radical cation of Chl a, formed upon the reduction of the substrate indole (**1a**). Borg *et al.* and other groups have shown that the pi radical cation of chlorophyll a generates an epr signal with $g = 2.0025 \pm 0.0001$ and epr line width = 7–13 Gauss, with Gaussian line shape, and absence of hyperfine splitting.³⁵ On the other hand, the indolyl radical-DMPO adducts could not be detected in the ESR spectrum (Fig. FS13, ESI[†]).

A plausible mechanism for the visible light mediated aerobic oxidation of indoles is proposed in Scheme 2. At first, the photocatalyst (Chl) transforms into its excited state Chl* under the irradiation of visible light; next, a photoinduced electron transfer (PET) from Chl* to **1** lead to a radical anion **I** and oxidized Chl⁺⁺ (confirmed by fluorescence quenching, ESR studies). Unlike transition metal polypyridyl complexes, the electron originates from the aromatic pi-electron system of the porphyrinic chromophore of the Chl molecule and not from the (closed shell element) Mg²⁺ ion.¹² However, Mg²⁺ ion is required for the structural and functional integrity of Chls,³⁶ and it is also found to be necessary for effective functioning of Chls in the present method (de-metallation of Chls was performed and subsequent reaction with crude pheophytin resulted in 15% yield of **2a**, see FS15, ESI[†]). Although there are very few reports on the single electron reduction of the indole moiety,³⁷ mechanistic investigation (*viz.* fluorescence quenching, ESR spectroscopy, CV data) strongly indicated the generation of an indole radical anion (**I**) *via* PET. The nucleophilicity of the indole ring is enhanced on being converted to the indole radical anion, which easily reacts with the singlet oxygen giving rise to the aminium radical ion (**II**). The aminium ion intermediate in turn donates an electron to Chl⁺⁺, affording a zwitterionic species (**III**) with the regeneration of the photocatalyst (Chl). Moreover, a radical chain propagation reaction *via* SET may also lead to species (**III**). Next, the zwitterionic species (**III**) forms a dioxetane intermediate (**IV**), which upon subsequent oxidative cleavage affords the product *N*-acetylacetaminophenone (**2**). Similarly, in the case of substrate **1B**, the dioxetane intermediate (**IV**) undergoes cleavage to keto amide (**V**), which upon Camps cyclization under basic conditions delivered the fused quinolin-4-ones (**3**). Furthermore, in the case of substrates **1C**, **1D** ($R^1 = H$), zwitterionic species (**III**) lead to the formation of the indoline-3-one intermediate **VI**, which undergoes nucleophilic attack by the indole substrate at the C-2 position giving intermediate **VII**.

Next, with substrate **1C** ($R^2 = Me/Ph$), the intermediate **VII** provides the monoindolylated product **4** under basic conditions. However, in the case of substrate **1D** ($R^2 = H$), intermediate **VII** yields species **VIII**, which upon SET with singlet

oxygen provides intermediate **IX** and O₂^{•-}. After that, the intermediate **IX** undergoes oxidation providing another iminium intermediate **X**, which upon further attack by the indole moiety afford the product 2,2-bis(indol-3-yl)indolin-3-ones (**5**).

Conclusion

We demonstrated the auto-tandem photocatalysis by crude chlorophyll and its mechanistic understanding. The photocatalytic process served as an efficient, green method towards the C-2,3 substitution-dependent oxidative transformation of indoles to afford oxidative cleavage products such as 2'-*N*-acetylaminacetophenones, tetrahydroacridin-9-ones, and dearomatized products such as 2-indolyl-3-oxindoles and 2,2-bis(indol-3-yl)indolin-3-ones. The chlorophyll in the crude form is an environmentally benign, cost-effective, and ubiquitous photocatalyst and probably bears the potential to achieve sustainability needs. Further exploration of the photocatalytic transformations using crude chlorophyll as the photocatalyst is currently underway.

Conflicts of interest

The authors declare no competing financial interest.

Acknowledgements

S. B. and S. C. are thankful to UGC, New Delhi, and G. P. is thankful to CSIR, New Delhi, India for financial assistance. The authors are thankful to SAIF-CDRI, Lucknow, India for providing spectral and analytical data. This work was supported in part by CSIR project MLP0123. The authors are grateful to Instrumentation Facility, UGC-DRS II, DST-FIST & DST-PURSE Assisted, Department of Chemistry, Aligarh Muslim University (AMU), Aligarh, India for providing ESR and CV Data. This is CSIR-CDRI communication no. 10212.

Notes and references

- (a) G. Ciamician, *Science*, 1912, **36**, 385–394; (b) H. D. Roth, *Angew. Chem., Int. Ed. Engl.*, 1989, **28**, 1193–1207.
- (a) A. Albini and M. Fagnoni, *Green Chem.*, 2004, **6**, 1; (b) C. R. Lhermitte and K. Sivula, *ACS Catal.*, 2019, **9**, 2007–20017.
- W. Liu, J. Li, P. Querard and C. J. Li, *J. Am. Chem. Soc.*, 2019, **141**, 6755–6764.
- (a) S. Protti and M. Fagnoni, *Photochem. Photobiol. Sci.*, 2009, **8**, 1499–1516; (b) V. Balzani, G. Bergamini and P. Ceroni, *Angew. Chem., Int. Ed.*, 2015, **54**, 11320–11337.
- (a) T. P. Yoon, M. A. Ischay and J. Du, *Nat. Chem.*, 2010, **2**, 527–532; (b) B. König, *Eur. J. Org. Chem.*, 2017, 1979–1981.
- (a) N. A. Romero and D. A. Nicewicz, *Chem. Rev.*, 2016, **116**, 10075–10166; (b) Q.-Q. Zhou, Y.-Q. Zou, L.-Q. Lu and W.-J. Xiao, *Angew. Chem., Int. Ed.*, 2018, **57**, 2–21.

- 7 (a) L. Huang and J. Zhao, *Chem. Commun.*, 2013, **49**, 3751–3753; (b) S. Guo, H. Zhang, L. Huang, Z. Guo, G. Xiong and J. Zhao, *Chem. Commun.*, 2013, **49**, 8689–8691; (c) J. Zhao, W. Wu, J. Sun and S. Guo, *Chem. Soc. Rev.*, 2013, **42**, 5323–5351; (d) D. P. Hari, P. Schroll and B. König, *J. Am. Chem. Soc.*, 2012, **134**, 2958–2961.
- 8 (a) G. O. Schenck and K. Ziegler, *Naturwissenschaften*, 1944, **32**, 157–157; (b) L. X. Chen, *Proc. Natl. Acad. Sci. U. S. A.*, 2020, **117**, 8672–8673; (c) S. Zhu and D. Wang, *Adv. Energy Mater.*, 2017, **7**, 1700841.
- 9 F. Strieth-Kalthoff, M. J. James, M. Teders, L. Pitzer and F. Glorius, *Chem. Soc. Rev.*, 2018, **47**, 7190–7202.
- 10 V. Dogra and C. Kim, *Front. Plant Sci.*, 2020, **10**, 1640.
- 11 (a) P. Roat, B. K. Malviya, S. Hada, B. Chechani, M. Kumar, D. K. Yadav and N. Kumari, *ChemistrySelect*, 2020, **5**, 9714–9719; (b) S. Harsh, S. Kumar, R. Sharma, Y. Kumar and R. Kumar, *Arabian J. Chem.*, 2020, **13**, 4720–4730; (c) A. Moazzam and F. Jafarpour, *New J. Chem.*, 2020, **44**, 16692–16696.
- 12 (a) S. Shanmugam, J. Xu and C. Boyer, *Chem. Sci.*, 2015, **6**, 1341–1349; (b) C. Wu, S. Shanmugam, J. Xu, J. Zhu and C. Boyer, *Chem. Commun.*, 2017, **53**, 12560–12563.
- 13 W. Schilling, Y. Zhang, P. K. Sahoo, S. K. Sarkar, S. Gandhi, H. W. Roesky and S. Das, *Green Chem.*, 2021, **23**, 379–387.
- 14 J. T. Guo, D. C. Yang, Z. Guan and Y. H. He, *J. Org. Chem.*, 2017, **82**, 1888–1894.
- 15 (a) M. Kobayashi, S. Ohashi, K. Iwamoto, Y. Shiraiwa, Y. Kato and T. Watanabe, *Biochim. Biophys. Acta, Bioenerg.*, 2007, **1767**, 596–602; (b) D. Nicewicz, H. Roth and N. Romero, *Synlett*, 2015, **27**, 714–723; (c) V. V. Pavlishchuk and A. W. Addison, *Inorg. Chim. Acta*, 2000, **298**, 97–102.
- 16 D. A. Hartzler, D. M. Niedzwiedzki, D. A. Bryant, R. E. Blankenship, Y. Pushkar and S. Savikhin, *J. Phys. Chem. B*, 2014, **118**, 7221–7232.
- 17 (a) B. Witkop and S. Goodwin, *J. Am. Chem. Soc.*, 1953, **75**, 3371–3376; (b) I. Saito, S. Matsugo and T. Matsuura, *J. Am. Chem. Soc.*, 1979, **101**, 7332–7338; (c) C. Zhang, S. Li, F. Bureš, R. Lee, X. Ye and Z. Jiang, *ACS Catal.*, 2016, **6**, 6853–6860.
- 18 (a) W. E. Knox and A. H. Mehler, *J. Biol. Chem.*, 1950, **187**, 419–430; (b) M. Mentel and R. Breinbauer, *Curr. Org. Chem.*, 2007, **11**, 159–176.
- 19 W. Pfrenge, T. Pachur, T. Nicola and A. Duran, *Pat*, WO2006048427, 2006.
- 20 (a) H. Hiyoshi and M. Ogawa, *Pat*, WO2002032882A1, 2002; (b) W. Jary, C. Rogl and W. Skranc, *Pat*, WO2007039034A1, 2007.
- 21 J. Xu, L. Liang, H. Zheng, Y. R. Chi and R. Tong, *Nat. Commun.*, 2019, **10**, 1–11.
- 22 (a) D. Anand, O. P. S. Patel, R. K. Maurya, R. Kant and P. P. Yadav, *J. Org. Chem.*, 2015, **80**, 12410–12419; (b) M. Ravi, P. Chauhan, S. Singh, R. Kant and P. P. Yadav, *RSC Adv.*, 2016, **6**, 48774–48778; (c) R. K. Maurya, O. P. S. Patel, D. Anand and P. P. Yadav, *Org. Chem. Front.*, 2018, **5**, 1170–1175; (d) S. Singh, P. Chauhan, M. Ravi and P. P. Yadav, *New J. Chem.*, 2018, **42**, 6617–6620.
- 23 A. R. Wellburn, *J. Plant Physiol.*, 1994, **144**, 307–313.
- 24 Y. Zhao, T. Meier, W. M. Zhang, V. Chernyak and S. Mukamel, *J. Phys. Chem. B*, 1999, **103**, 3954–3962.
- 25 (a) E. Ucar, N. Caglayan and K. Turgut, *Not. Sci. Biol.*, 2016, **8**, 354–359; (b) T. Kon and T. Kusano, *Opt. Photonik*, 2014, **9**, 62–65.
- 26 (a) S. Hortensteiner, *Annu. Rev. Plant Biol.*, 2006, **57**, 55–77; (b) C. A. Llewellyn, R. Fauzi, C. Mantoura and R. G. Brereton, *Photochem. Photobiol.*, 1990, **52**, 1043–1047.
- 27 (a) S. Pradhan, C. K. Shahi, A. Bhattacharyya, N. Chauhan and M. K. Ghorai, *Org. Lett.*, 2017, **19**, 3438–3441; (b) P. P. Varma, B. S. Sherigara, K. M. Mahadevan and V. Hulikal, *Synth. Commun.*, 2008, **39**, 158–165.
- 28 R. M. Cross, J. R. Maignan, T. S. Mutka, L. Luong, J. Sargent, D. E. Kyle and R. Manetsch, *J. Med. Chem.*, 2011, **54**, 4399–4426.
- 29 J. Warneke and E. Winterfeldt, *Chem. Ber.*, 1972, **105**, 2120–2125.
- 30 L. A. Mitscher, *Chem. Rev.*, 2005, **105**, 559–592.
- 31 S. K. Guchhait, V. Chaudhary, V. A. Rana, G. Priyadarshani, S. Kandekar and M. Kashyap, *Org. Lett.*, 2016, **18**, 1534–1537.
- 32 S. B. Gohain, M. Basumatary, P. K. Boruah, M. R. Das and A. J. Thakur, *Green Chem.*, 2020, **22**, 170–179.
- 33 (a) J. Kothandapani, S. M. K. Reddy, S. Thamocharan, S. M. Kumar, K. Byrappa and S. S. Ganesan, *Eur. J. Org. Chem.*, 2018, 2762–2767; (b) G. Shukla, A. Dahiya, T. Alam and B. K. Patel, *Asian J. Org. Chem.*, 2019, **8**, 2243–2248; (c) C. Ganachaud, V. Garfagnoli, T. Tron and G. Iacazio, *Tetrahedron Lett.*, 2008, **49**, 2476–2478.
- 34 (a) T. Entradas, S. Waldron and M. Volk, *J. Photochem. Photobiol., B*, 2020, **204**, 111787; (b) J. Ye, J. Wu, T. Lv, G. Wu, Y. Gao and H. Chen, *Angew. Chem., Int. Ed.*, 2017, **56**, 14968–14972.
- 35 (a) D. C. Borg, A. Forman and J. Fajer, *J. Am. Chem. Soc.*, 1976, **98**, 6889–6893; (b) D. C. Borg, J. Fajer, R. H. Felton and D. Dolphin, *Proc. Natl. Acad. Sci. U. S. A.*, 1970, **67**, 813–820; (c) J. Fajer, D. C. Borg, A. Forman, D. Dolphin and R. H. Felton, *J. Am. Chem. Soc.*, 1970, **92**, 3451–3459.
- 36 (a) L. Fiedor, A. Kania, B. Myśliwa-Kurczel, Ł. Orzeł and G. Stochel, *Biochim. Biophys. Acta, Bioenerg.*, 2008, **1777**, 1491–1500; (b) L. Fiedor, V. Rosenbach-Belkin and A. Scherz, *J. Biol. Chem.*, 1992, **267**, 22043–22047; (c) M. S. Fischer, D. H. Templeton, A. Zalkin and M. Calvin, *J. Am. Chem. Soc.*, 1972, **94**, 3613–3619; (d) K. M. Barkigia and D. S. Gottfried, *Acta Crystallogr., Sect. C: Cryst. Struct. Commun.*, 1994, **50**, 2069–2072.
- 37 (a) D. Bandyopadhyay, I. Biswas, S. Laskar and B. Basak, *Int. J. Pharm. Pharm. Sci.*, 2013, **5**, 447–450; (b) A. Banerji, D. Bandyopadhyay, B. Basak, P. K. Biswas, J. Banerji and A. Chatterjee, *Chem. Lett.*, 2005, **34**, 1500–1501; (c) T. Saget and B. Koenig, *Chem. – Eur. J.*, 2020, **26**, 7004–7007; (d) Y. Xiao, S.-E. Zhu, D.-J. Liu, M. Suzuki, X. Lu and G.-W. Wang, *Angew. Chem., Int. Ed.*, 2014, **53**, 3006–3010; (e) G. H. Naik, K. I. Priyadarsini and H. Mohan, *Phys. Chem. Chem. Phys.*, 2002, **4**, 5872–5877.